



24th COBEM - 2017



24th ABCM International Congress of Mechanical Engineering
December 3-8, 2017, Curitiba, PR, Brazil

COBEM-2017-2093

NUMERICAL ANALYSIS OF NATURAL CONVECTION HEAT TRANSFER ON AIR-COOLED FINNED TUBES

Rayanne Carla Alves do Nascimento

Sandi Itamar Schafer de Souza

Universidade Federal do Rio Grande do Norte. Av. Sen. Salgado Filho, 3000 - Lagoa Nova, Natal - RN, 59064-741
rayannecarla@gmail.com, sandi@ufrnet.br

Abstract. *The objective of this study is to investigate the natural convection heat transfer from air-cooled finned tubes on a horizontal cylinder. For the CFD simulations, surrounding air temperature is varied from 22°C to 33°C and the fin base temperature from 8°C to 15°C. Heat transfer rates from fin interfaces and tube base are calculated through the simulations, and good agreement is observed. The effects of fin diameter and ambient to surface temperature difference on the heat transfer have been investigated. The effectiveness of the fins was also evaluated for all the CFD simulations.*

Keywords: *natural convection, finned tube, laminar flow, Nusselt Number, annular fin*

1. INTRODUCTION

Fins are widely applicable on refrigeration of combustion engines, of electric power transformers, of electric motors and on heat exchangers on air-conditioning systems. These are part of the problems that exist in industry in the area of heat transfer. Thus it is noticed that there is relevance of studying the phenomena that encompass the behavior and the efficiency of the devices that are responsible for the heat transfer.

Natural convection happens due to a density gradient and are induced by buoyancy force. As the velocities existing in a natural convection flow are much lower than those that act in forced convection, heat transfer rates on free convection are also much lower. However forced convection is much expensive than the natural convection due to the equipments that are necessary to promote the fluid flow. So when it is necessary to minimize the operating costs air-cooled finned tubes are largely used. Since the simple use of fins does not guarantee an increase of the heat transfer, an investigation can be done by evaluating the effectiveness of the fin. (Incropera, F. P. and DeWitt, D. P., 2008)

The classical heat transfer literature presents the equations for the design for numerous configurations. The design of radial fins is part of the group of non-uniform straight section fins and it is the one studied in this work. Some important simplifications are used according to the design. One of them is the use of a constant convective coefficient on the fin. However, it is known that the fluid flow and the presence of the tube base create a complex flow around the solid. The determination of the convective coefficient depends on the geometry. And it can cause the adoption of additional simplifying hypotheses. In the determination of effectiveness, the literature assumes that the convective coefficient acting on the fin is equivalent to that at its base, neglecting the effects of the fins on the convective coefficient. The coefficient of heat transfer in the wall of the tube is considered constant. However, it is known that it varies radially and axially. Therefore these considerations distance the results of physical reality. (Souza, S. I. S. and Bessa, K. L., 2016)

Kayansayan and Karabacak (1992) developed experimental studies on finned tubes. The authors investigated the behavior of the Nusselt number as a function of Rayleigh, that is, the effect of the spacing on the convective coefficient. For low values of spacing, the results showed that a presence of the fins interferes strongly on the convective coefficient. Hahne and Zhu (1994) conducted experiments to identify the effect of height on the heat transfer process. The results found for the Nusselt number were similar to those obtained by correlations. Chen and Hsu (2007) investigated thermal exchange using an inverse problem technique associated with experimental results. In this work the results of the medium convective coefficient heat transfer and the efficiency according to the fin spacing are presented. Yaghoubi and Mahdavi (2013) developed an experimental numerical work with the objective of investigating the natural convection of tubes with aluminum fins used to cool the surrounding air. The physical dimensions were kept constant. The temperature of the environment and the base of the tube were controlled. The results of the velocity field and the convective coefficient as a function of the ambient temperature and the temperature of the base are presented.

Kumar et al. (2016) developed numerical 3D studies on the subject. They evaluated the effect of fin spacing, fin diameter and the fin-environment temperature difference on the thermal changes and thrust forces generated. Senapati et al. (2016) also developed a numerical study about this subject with industrial relevance. They evaluated the effects of the relation between the fin spacing and diameter (S/d) over the heat flux, efficiency and temperature plume through correlations. The results show that at low values of S/d the fin efficiency decreases rapidly and remains almost constant for higher S/d values. They also show that the heat transfer attains a maxima in some point as the S/d relations grows and then starts to decrease.

As a result of the high costs of experimental procedures and good experiences with the numerical simulations, CFD simulations have become a notable alternative for the study of heat transfer. Several studies of natural convection heat transfer on finned tubes were previously conduct and are listed in the references.

2. COMPUTACIONAL PROCEDURE

In the present work will be created computational models similar to those studied in the experimental work of Yaghoubi and Mahdavi (2013) with the support of a commercial program of Computational Fluid Dynamics, Ansys CFX®. Initially the case will be studied with the same dimensions to be used as validation of the simulations. The diameter of the fins will then be changed. For each new situation, 9 cases will be simulated, varying the surrounding air temperature (22°C, 25°C and 33°C) and wall temperature (8°C, 12°C and 15°C). The influence of the external fin diameter on the convective coefficient of heat transfer will also be studied varying the relation between external and internal diameters of the fins.

The meshes are created through a simplified geometry of the heat exchanger seen in Fig. 1. They were generated with the support of ICEM CFD 13.0. The geometry shown in Fig. 1 was created with the support of the Design Modeling, Ansys drawing package. The measurements shown in the figure have the following values $d_i = 25.4$ mm, $D_f = 56, 80$ and 100 mm, $L = 3D_f$, $H = 7D_f$, $S = 2$ mm and $t = 0.4$ mm. Where d_i and D_f are respectively the internal and external diameters of the fin, L and H are respectively the width and height of the fluid domain, S is the spacing between the fins, and t the thickness of the fin. In simplified geometry, t is used in half and L is already half the width of the total fluid domain.

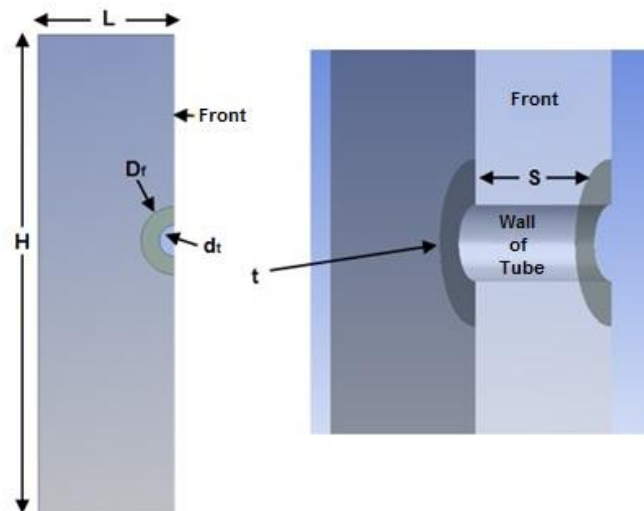


Figure 1. Simplified geometry used for the generation of meshes

The boundary conditions used were air as ideal gas in the fluid domain; fins of aluminum in the solid domain; the sides and the front of the fluid domain were considered by symmetry; the back of the fluid domain was considered adiabatic and no slip wall; the top and bottom of the fluid domain were considered as an opening boundary at the following temperatures $T_{air} = 22^\circ\text{C}$, 27°C and 33°C ; in the tube and fin bases, the following temperatures were considered $T_{sur} = 8^\circ\text{C}$, 12°C and 15°C . The convergence criterion used was RMS of 1.0×10^{-6} for all speeds and pressures, where RMS is a statistical measure of the magnitude of the root mean square value of a variable quantity. The advection scheme used was Upwind and the total buoyancy model was applied.

The Rayleigh number was used to observe the behavior of air flow over the geometry, Eq. (1). The values obtained were of the order of magnitude of 3.0×10^5 , implying in a laminar flow for all simulated situations.

$$Ra_D = \frac{g\beta(T_{air} - T_{sur})D_f^3}{\nu\alpha} \quad (1)$$

Where g is the gravity, D_f is the characteristic plate length, β , ν and α are, respectively, the coefficient of thermal expansion, kinematic viscosity and thermal diffusivity calculated at the film temperature $T_f = (T_{air} + T_{sur})/2$. T_{air} is the air temperature and T_{sur} is the set temperature of the tube surface.

For the modeling of the laminar flow, it was needed to apply the momentum equation and the conservation equations of energy and mass in the index form and only for the x axis, Eq. (2), (3) and (4) respectively. The effects on the y and z axes are negligible. The Eq. (5) is the equation for the solution of equation of energy to the solid domain representing the diffusion of the heat through the fins.

$$\frac{\partial}{\partial x_j} (\rho U_i U_j) = -\frac{\partial p}{\partial x_i} + \frac{\partial}{\partial x_j} \left[\mu \left(\frac{\partial U_i}{\partial x_j} + \frac{\partial U_j}{\partial x_i} \right) \right] + S_M \quad (2)$$

$$\frac{\partial}{\partial x_j} (\rho U_j T) = \frac{\partial}{\partial x_j} \left(\frac{k}{c_p} \frac{\partial T}{\partial x_j} \right) \quad (3)$$

$$\frac{\partial}{\partial x_j} (\rho U_j) = 0 \quad (4)$$

$$\frac{\partial}{\partial x_j} \left(k \frac{\partial T}{\partial x_j} \right) = 0 \quad (5)$$

2.1 Control of Numerical Accuracy

In computational fluid dynamics studies, one of the main concerns is to detect, estimate and control the numerical uncertainty and error associated with the simulations. The method used for the discretization of the error estimation was the Richardson extrapolation (RE). This is currently the most robust method available for predicting numerical uncertainty.

This procedure recommends five steps to estimate the discretization of the error. The first step is to define a representative cell, variable based on the settings of the mesh with size h . As this study is based on a 3D geometry, the variable h is defined by Eq. (6).

$$h = \left[\frac{1}{N} \sum_{i=1}^N (\Delta V_i) \right]^{1/3} \quad (6)$$

where ΔV_i is the volume of the i^{th} cell, and N is the total number of cells used in the simulations.

The second step is to select three significantly set of grids, and run simulations to determine the values of some key variable important to the objective of the simulation study (ϕ). At this study, the critical variable reported was the heat flux. It is desirable that the grid refinement factor, $r = h_{\text{coarse}}/h_{\text{fine}}$, be greater than 1.3. This value is based on experience, and not on formal derivation.

The third step is to set $h_1 < h_2 < h_3$, calculate $r_{21}=h_2/h_3$ and $r_{32}=h_3/h_2$, and generate the apparent order p , using Eq. (7), (8) and (9).

$$p = \frac{1}{\ln(r_{21})} |\ln|\epsilon_{32}/\epsilon_{21}| + q(p)| \quad (7)$$

$$q(p) = \ln \left(\frac{r_{21}^p - s}{r_{32}^p - s} \right) \quad (8)$$

$$s = 1 \cdot \text{sign}(\epsilon_{32}/\epsilon_{21}) \quad (9)$$

where $\epsilon_{32} = \phi_3/\phi_2$, $\epsilon_{21} = \phi_2/\phi_1$, ϕ_j denoting the solution of the j^{th} grid.

The fourth step is to calculate the extrapolated values, Eq. (10).

$$\phi_{\text{ext}}^{21} = (r_{21}^p \phi_1 - \phi_2) / (r_{21}^p - 1) \quad (10)$$

Similarly, calculate ϕ_{ext}^{32} .

The fifth step is to calculate and report the following error estimates, Eq. (11), (12) and (13).

$$e_a^{21} = \left| \frac{\phi_1 - \phi_2}{\phi_1} \right| \quad (11)$$

$$e_{\text{ext}}^{21} = \left| \frac{\phi_{\text{ext}}^{12} - \phi_2}{\phi_{\text{ext}}^{12}} \right| \quad (12)$$

$$\text{GCI}_{\text{fine}}^{21} = \frac{1.25 e_a^{21}}{r_{21}^p - 1} \quad (13)$$

Table 1 shows the results for this calculation for three selected grids with a total number of cells N_1 , N_2 and N_3 . Hence, according to Tab. 1, the numerical uncertainty in the fine-grid solution for the heat flux should be reported as 0.35%.

Table 1. Sample calculations of discretization error

ϕ=heat flux through the fins and wall tube	
N_1, N_2, N_3	237600, 70800, 19500
r_{21}	1.50
r_{32}	1.54
ϕ_1	0.03372
ϕ_2	0.03422
ϕ_3	0.03787
p	4.5762
ϕ_{ext}^{21}	0.03362
e_a^{21}	1.5%
e_{ext}^{21}	0.28%
$\text{GCI}_{\text{fine}}^{21}$	0.35%

3. RESULTS AND DISCUSSION

In Tab. 2, 3, 4 and 5, convective coefficients of heat transfer and heat flux per area for each diameter are shown in their nine configurations of temperature difference between environment and tube surface. It is noted that increasing the diameter promotes an increase in the heat flux transferred by the fins. In addition, the convective coefficient of heat transfer decreases significantly with each configuration change. Statistically, the increase in heat flux for each of the nine configurations of temperature difference between environment and surface of the tube is between 37 and 48% when changing D_f from 56 to 80 mm and between 20 and 27% when changing D_f from 80 to 100 mm. The overall increase in heat flux when changing D_f from 56 to 100 mm reaches a level between 70 and 89%. In Tab. 2 and 3, the convective coefficients of heat transfer are specified in $\text{W}/\text{m}^2\text{C}$. In Tab. 2, the subscript of h indicates the fin diameter. In Tab. 4 and 5, the heat flux per area is specified in W/m^2 . The convective coefficient of heat transfer was calculated through Eq. (14), where h is the convective coefficient of heat transfer, A is the sum of the heat exchange area of tube and fin surfaces and q represents the heat flux between tube and air, obtained numerically through simulation.

$$h = \frac{q}{A(T_{\text{air}} - T_{\text{sur}})} \quad (14)$$

Table 2. Comparison of the convective coefficient of heat transfer for the three different diameters of the fins (D_f)

	$T_{sur} = 8^\circ\text{C}$			$T_{sur} = 12^\circ\text{C}$			$T_{sur} = 15^\circ\text{C}$		
	h_{56}	h_{80}	h_{100}	h_{56}	h_{80}	h_{100}	h_{56}	h_{80}	h_{100}
$T_{air} = 22^\circ\text{C}$	0.68	0.43	0.33	0.63	0.39	0.30	0.54	0.33	0.25
$T_{air} = 27^\circ\text{C}$	0.75	0.48	0.38	0.67	0.43	0.33	0.62	0.39	0.30
$T_{air} = 33^\circ\text{C}$	0.84	0.56	0.44	0.77	0.50	0.39	0.71	0.46	0.36

Table 3. Convective coefficient of heat flux of the tube without fins (d_t)

	$T_{sur} = 8^\circ\text{C}$	$T_{sur} = 12^\circ\text{C}$	$T_{sur} = 15^\circ\text{C}$
$T_{air} = 22^\circ\text{C}$	6.43	6.01	5.61
$T_{air} = 27^\circ\text{C}$	6.72	6.38	6.08
$T_{air} = 33^\circ\text{C}$	7.08	6.81	6.58

Table 4. Comparison of the heat flux per area for the three different diameters of the fins (D_f)

	$T_{sur} = 8^\circ\text{C}$			$T_{sur} = 12^\circ\text{C}$			$T_{sur} = 15^\circ\text{C}$		
	$(q/A)_{56}$	$(q/A)_{80}$	$(q/A)_{100}$	$(q/A)_{56}$	$(q/A)_{80}$	$(q/A)_{100}$	$(q/A)_{56}$	$(q/A)_{80}$	$(q/A)_{100}$
$T_{air} = 22^\circ\text{C}$	9.20	5.85	4.50	5.80	3.61	2.73	3.64	2.23	1.67
$T_{air} = 27^\circ\text{C}$	13.85	8.94	7.00	9.84	6.28	4.83	7.22	4.52	3.45
$T_{air} = 33^\circ\text{C}$	20.45	13.54	10.66	15.68	10.21	7.97	12.50	8.02	6.23

Table 5. Heat flux per area of the tube without fins (d_t)

	$T_{sur} = 8^\circ\text{C}$	$T_{sur} = 12^\circ\text{C}$	$T_{sur} = 15^\circ\text{C}$
$T_{air} = 22^\circ\text{C}$	90.07	60.10	39.28
$T_{air} = 27^\circ\text{C}$	127.64	95.72	73.00
$T_{air} = 33^\circ\text{C}$	177.12	142.99	118.44

In Fig. 2, the fin temperature field is shown for the case where the air (T_{air}) is at 33°C and the tube and fin surface (T_{sur}) at 8°C . The fin temperature field shows that the heat flux between the air and the fins produces a temperature gradient, so that the temperature on its surface is not constant. At its surface, the temperature is constant $T_{sur} = 8^\circ\text{C}$, varying radially and angularly. Moreover, it is perceived that the increase in D_f promotes a rise in temperature along the length of the fin.

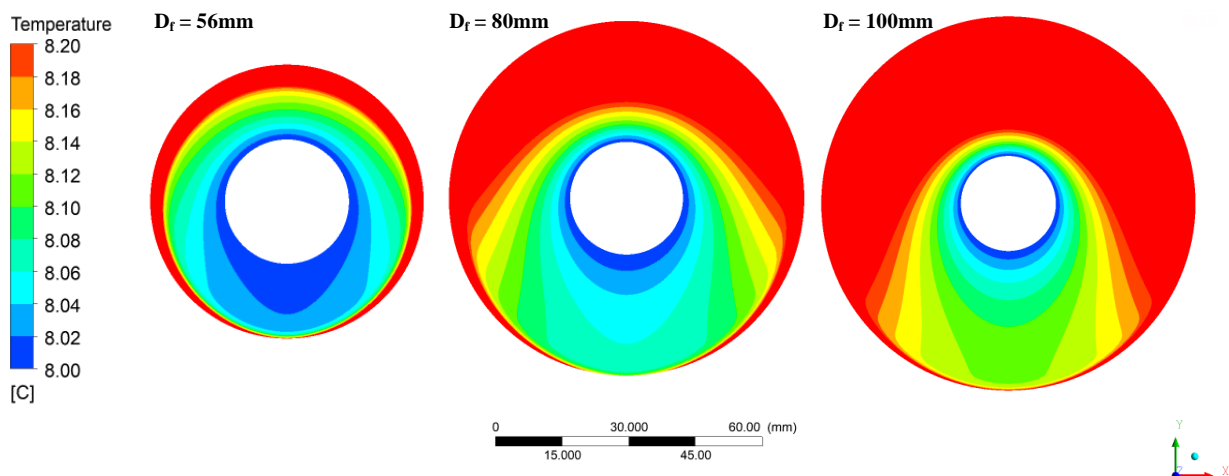


Figure 2. Fin temperature field, for the case where $T_{sur} = 8^\circ\text{C}$ and $T_{air} = 33^\circ\text{C}$.

In Fig. 3, velocity v field is shown for the case where the air (T_{air}) is at 33°C and the tube and fin surface (T_{sur}) at 8°C . It is noticed that in all the extension of the domains the speed of the air due to the natural ventilation is very low. In

addition, it is noted that in the region where the heat transfer between the fins and air actually occurs, the velocity is even lower than in the regions furthest from the fins. Concentrating around values below 0.05m/s.

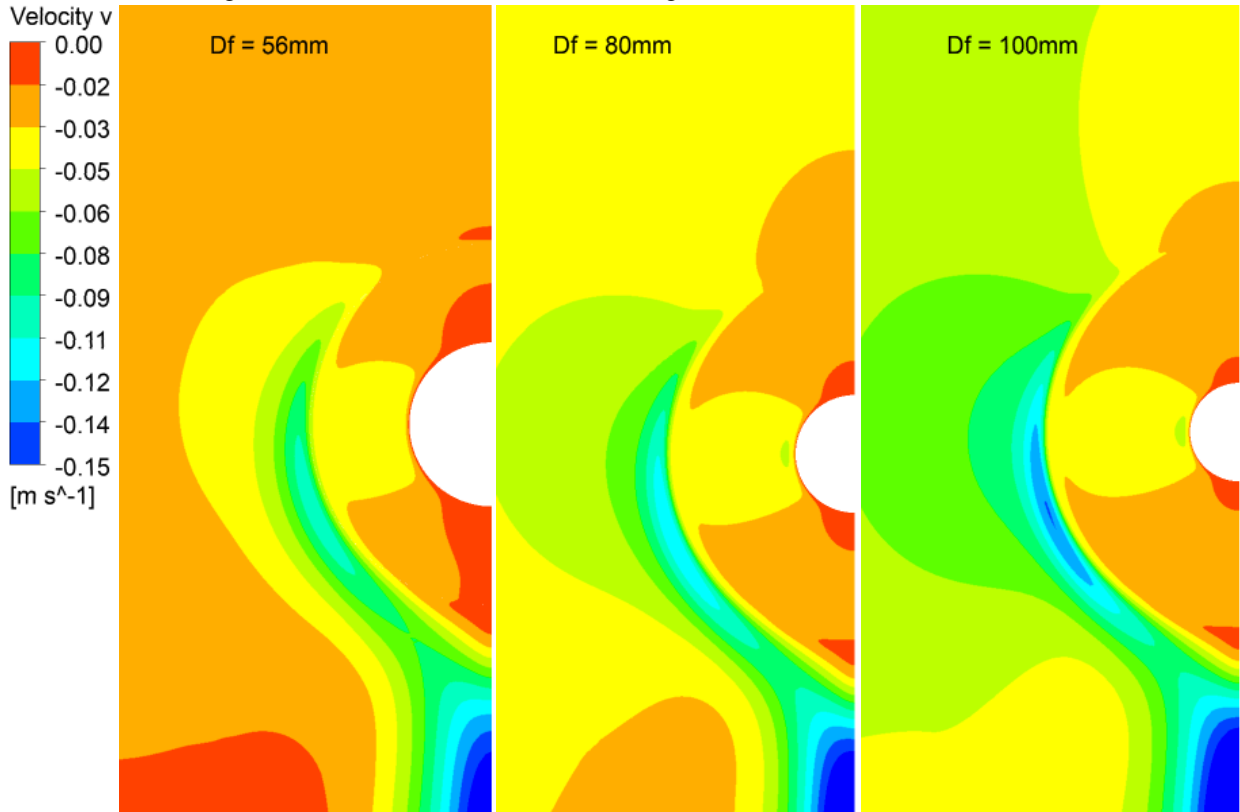


Figure 3. Velocity v field, for the case where $T_{sur} = 8^{\circ}\text{C}$ and $T_{air} = 33^{\circ}\text{C}$.

For the calculation of the effectiveness, it is necessary to quantify the convective coefficient of heat transfer without the presence of the fins. The heat transfer was simulated for a tube without fins and with external diameter of 25.4mm and length of 100mm. The dimensions of the simulated fluid domain H and L were 400mm and 200mm respectively. The boundary conditions of the finned tube were repeated for the tube without fins. Tab. 6 shows the results obtained for the numerical Nusselt number (Nu_1), obtained through Eq. (14) and (15), compared to the analytical values calculated by the correlation of Churchill and Chu (1975) - Nu_2 and Morgan (1975) - Nu_3 . Comparing the results, it is noticed that the maximum percentage error is within the acceptable, below 10%.

Table 6. Nusselt number for the tube without fins.

	$T_{sur} = 8^{\circ}\text{C}$			$T_{sur} = 12^{\circ}\text{C}$			$T_{sur} = 15^{\circ}\text{C}$		
	Nu_1	Nu_2	Nu_3	Nu_1	Nu_2	Nu_3	Nu_1	Nu_2	Nu_3
$T_{air} = 22^{\circ}\text{C}$	6.45	5.46	6.05	5.99	5.02	5.52	5.55	4.60	5.01
$T_{air} = 27^{\circ}\text{C}$	6.67	5.88	6.45	6.30	5.53	6.03	5.98	5.23	5.69
$T_{air} = 33^{\circ}\text{C}$	6.97	6.28	6.83	6.66	6.00	6.49	6.41	5.77	6.22

$$Nu = \frac{h D_f}{k_{air}} \quad (15)$$

where A in Eq. (14) is the heat exchange area of the tube and k_{air} is the thermal diffusivity coefficient of the air, considered constant.

The effectiveness of the fin is defined by the ratio between the heat transfer rate of the fin and the rate of heat transfer that would exist without the fin, Eq. (16). In Tab. 7, 8 and 9, it is placed the numerically calculated (ϵ_{fin}) values of effectiveness through the simulation results and analytically (ϵ_{fa}). Equation 17 is the analytical solution for the fin with non-uniform straight section area, with the temperature at the base being specified and the end presumed to be adiabatic.

$$\varepsilon_f = \frac{q_f}{h A_{tr,b} (T_\infty - T_{sur})} \quad (16)$$

$$q_f = 2\pi k r_1 t (T_\infty - T_{sur}) m \frac{K_1(mr_1)I_1(mr_{2c}) - I_1(mr_1)K_1(mr_{2c})}{K_0(mr_1)I_1(mr_{2c}) + I_0(mr_1)K_1(mr_{2c})} \quad (17)$$

$$m = \sqrt{\frac{2h_1}{kt}} \quad (18)$$

where q_f is the heat transferred through the fin, determined analytically and through the simulation results, and $A_{tr,b}$ is the area of the fin base. The h used in Eq. (16) should be the h of the tube without fin and h_1 is obtained through the simulations of the finned tube, Tab. 2. The terms K_0 and I_0 are the modified Bessel functions of order zero, first and second species, Incropera (2008). The terms K_1 and I_1 are the first order Bessel modified functions of first and second species, Incropera (2008). k is the thermal diffusivity coefficient of the fin material. The differences between the results of numerical and analytical effectiveness showed differences within the expected, below 10%.

Table 7. Effectiveness of the fin for $D_f = 56$ mm, calculated numerically through the results of the simulations and analytically through correlations.

	$T_{sur} = 8^\circ\text{C}$		$T_{sur} = 12^\circ\text{C}$		$T_{sur} = 15^\circ\text{C}$	
	ε_{fn}	ε_{fa}	ε_{fn}	ε_{fa}	ε_{fn}	ε_{fa}
$T_{air} = 22^\circ\text{C}$	27.21	27.58	27.33	28.21	24.76	26.14
$T_{air} = 27^\circ\text{C}$	28.85	28.35	27.36	27.14	26.34	26.37
$T_{air} = 33^\circ\text{C}$	30.68	29.74	29.16	28.43	28.09	27.53

Table 8. Effectiveness of the fin for $D_f = 80$ mm, calculated numerically through the results of the simulations and analytically through correlations.

	$T_{sur} = 8^\circ\text{C}$		$T_{sur} = 12^\circ\text{C}$		$T_{sur} = 15^\circ\text{C}$	
	ε_{fn}	ε_{fa}	ε_{fn}	ε_{fa}	ε_{fn}	ε_{fa}
$T_{air} = 22^\circ\text{C}$	38.80	40.16	38.19	40.25	34.08	36.77
$T_{air} = 27^\circ\text{C}$	41.80	41.90	39.16	39.66	37.06	37.89
$T_{air} = 33^\circ\text{C}$	45.61	45.06	42.64	42.40	40.43	40.44

Table 9. Effectiveness of the fin for $D_f = 100$ mm, calculated numerically through the results of the simulations and analytically through correlations.

	$T_{sur} = 8^\circ\text{C}$		$T_{sur} = 12^\circ\text{C}$		$T_{sur} = 15^\circ\text{C}$	
	ε_{fn}	ε_{fa}	ε_{fn}	ε_{fa}	ε_{fn}	ε_{fa}
$T_{air} = 22^\circ\text{C}$	48.09	49.93	46.51	49.21	40.85	44.49
$T_{air} = 27^\circ\text{C}$	52.74	53.00	48.54	49.32	45.50	46.70
$T_{air} = 33^\circ\text{C}$	57.86	57.25	53.62	53.44	50.61	50.76

4. CONCLUSION

The uncertainty associated with the meshes calculated by the RE method was sufficiently small, less than 1%. The results obtained with the simulations showed good agreement with the analysis of the natural convection in finned tubes and, because of this, that the numerical treatment through simulations is a good tool to predict physical behavior in this case. The results showed that for the situation where the fin spacing corresponds to 2mm, the heat transfer is of low intensity. Knowing that for any rationally dimensioned design the results of effectiveness should be the highest as possible, it is noticed that the use of fins for this application is advantageous, even though the heat transfer intensity is low for the configuration where $S = 2\text{mm}$, because $\varepsilon_f > 2$. The low intensity of the heat transfer is due to the low air velocity, characteristic of the natural convection. However, it is noticed that in the region between the fins the velocity is even smaller, very close to zero. This implies that the heat exchange for $S = 2\text{mm}$ occurs more by conduction than by convection, where the air acts as a thermal conductor. The temperature at the base of the fin were found to be constant and the behavior of its temperature field reveals that its variation occurs radially and angularly. The temperature variations in the fin are not high and as result the fin can be estimated as an isothermal surface. This low temperature

variation occurs due to the material considered in the analysis, pure aluminum, which presents a thermal diffusivity coefficient of the order of 237 W/mK. The convective coefficient of heat transfer depends strongly on the shape of the fin, since this is the form that is used to choose the correlations to be used in the analytical calculations. These correlations that take geometry approximations into account imprint uncertainties in the calculation process by taking analytical results away from numerical results. The increase in the fin diameter causes the reduction of the convective coefficient of heat transfer and increase the heat flux between the fins and the air as expected. However, through the statistical analysis of the increase of the heat flow with the increase of the fin diameter, it is noticed that this increase does not always occur in the same proportion. The larger the fin diameter gets, the lower is the increase of the heat flux between the previous and the next configuration. It shows that there is a limit size for the fin diameter, from which there is no further increase in the heat flow between the air and the fin. The effectiveness of the fin in relation to the increase of the fin diameter follows that one of the heat flux.

5. ACKNOWLEDGEMENTS

This work was supported by PRH ANP – 14 and by Laboratório de Dinâmica de Fluidos Computacional – UFRN.

6. REFERENCES

- ASME, 2008. "Procedure for Estimation and Reporting of Discretization Error in CFD Applications". 2 Sep. 2017 < <http://fluidsengineering.asmedigitalcollection.asme.org/article.aspx?articleid=1434171>>.
- Chen, H. and Hsu, W., 2007. "Estimation of heat transfer coefficient on the fin of annular-finned tube heat exchangers in natural convection for various fin spacings". *International Journal of Heat and Mass Transfer*, Vol. 50, p. 1750-1761.
- Churchill, S.W. and Chu, H.H.S., 1975. "Correlating Equations for Laminar and Turbulent Free Convection from Horizontal Cylinder". *International Journal of Heat and Mass Transfer*, Vol. 18, p. 1049-1053.
- Incropera, F. P. and DeWitt, D. P., 2008. *Fundamentos de Transferência de Calor e de Massa*. LTC, Rio de Janeiro, 6th edition.
- Hahne, E. and Zhu, D., 1994. "Natural convection heat transfer on finned tubes in air". *International Journal of Heat and Mass Transfer*, vol. 37, p. 59-63.
- Kayansayan, N. and Karabacak, R., 1992. "Natural convection heat transfer coefficients for a horizontal cylinder with vertically attached circular fins". *Heat Recovery Systems & CHP*, vol. 12, p. 457-468.
- Kumar, et. al., 2016. "3D CFD simulations of air cooled condenser-II: Natural draft around a single finned tube kept in a small chimney". *International Journal of Heat and Mass Transfer*, vol. 92, p. 507-522.
- Kumar, et. al., 2016. "3D numerical study of the effect of eccentricity on heat transfer characteristics over horizontal cylinder fitted with annular fins". *International Journal of Thermal Sciences*, vol. 108, p. 28-39.
- Senapati et al., 2016. "Numerical investigation of natural convection heat transfer over annular finned horizontal cylinder". *International Journal of Heat and Mass Transfer*, vol. 96, p. 330-345.
- Souza, S. I. S. and Bessa, K. L., 2016. "Numerical Simulation of Natural Convection Heat Transfer in Circular Fins". In *Proceedings of 16th Brazilian Congress of Thermal Sciences and Engineering - ENCIT2016*. Vitória, Brazil.
- Yaghoubi, M. and Mahdavi, M., 2013. "An investigation of natural convection heat transfer from a horizontal cooled finned tube". *Experimental Heat Transfer*, vol. 26, p. 343-359.

7. RESPONSIBILITY NOTICE

The authors are the only responsible for the printed material included in this paper.